Journal of Applied Pharmaceutical Research
Volume 14 Issue 1, Year of Publication 2026, Page 31 – 41
DOI: https://doi.org/10.69857/joapr.v14i1.1377

Check for updates

Research Article

JOURNAL OF APPLIED PHARMACEUTICAL RESEARCH | ***JOAPR***
www.japtronline.com ***ISSN: 2348 – 0335***

DEVELOPMENT AND CHARACTERIZATION OF NANOCRYSTALS FOR SOLUBILITY ENHANCEMENT OF POORLY SOLUBLE DRUG AZELNIDIPINE

Sandeep D. Kardile*, Vipul P. Patel

Article Information
Received: 7th September 2025
Revised: 16th November 2025
Accepted: 11th December 2025
Published: 5th January 2026

Keywords
Azelnidipine, Solubility, Dissolution, Nanocrystals, Antihypertensive.

ABSTRACT

Background: Azelnidipine is a BCS Class II drug characterized by low solubility and high permeability, resulting in approximately 50% bioavailability. The limited bioavailability of this compound is primarily attributed to its poor aqueous solubility. Therefore, enhancing the solubility and dissolution rate of Azelnidipine is essential to improve its bioavailability. This study aimed to develop and characterize Azelnidipine Nanocrystals to enhance the solubility and dissolution rate of Azelnidipine, which is currently in micronized form. **Methodology:** Azelnidipine nanocrystals were prepared via antisolvent precipitation. Azelnidipine nanocrystals were synthesized using PVP and SLS as stabilizers via a precipitation process. Saturation solubility was tested in 5 mL of 0.1 N HCl and in phosphate buffers at pH 6.8 and 7.4. The physicochemical properties of the nanocrystals, including physical appearance, FTIR, DSC, SEM, XRD, solubility, particle size distribution, zeta potential, and in vitro drug release, were evaluated. **Results and Discussion:** FTIR spectroscopy confirmed drug compatibility and ruled out potential interactions with the polymers. Nine nanocrystal formulations (F1 to F9) containing pure Azelnidipine in micronized form with varying percentages of PVP and SLS stabilizers were tested. In batches F1 to F3, the drug-to-polymer PVPK30 ratio was 1:1, and the SLS concentration was increased by 0.05, 0.10, and 0.150, yielding the highest drug release in batch F3 (97.68%). The study found that as SLS concentration increased, solubility increased; similarly, as particle size decreased, solubility increased. **Conclusion:** Conversion of the micronized form of Azelnidipine to the nanocrystal form increases its solubility.

INTRODUCTION

Nanotechnology offers great potential for the formulation and development of novel and existing pharmaceuticals. It reduces the drug's particle size to nanoscale dimensions, thereby improving its physical characteristics [1]. The goal of nanotechnology is to develop novel drug formulations, such as nanocrystals of BCS Class II drugs. The creation of nanocrystals improves the bioavailability and solubility of poorly soluble

*Sanjivani College of Pharmaceutical Education and Research, Savitribai Phule Pune University, Pune, Kopargaon, Dist. Ahilya Nagar, Maharashtra, India -42360

For Correspondence: **sandeepkardile9970@gmail.com**

therapeutic candidates and helps ensure their safety and effectiveness [2]. Many complex drug molecules exhibit high affinity for their targets but low solubility. Drugs with poor water solubility pose a significant challenge in formulation and development. Approximately 40% of marketed medications and 90% of drug candidates are classified as poorly water-soluble, highlighting a growing issue. Nanoformulations, such as nanocrystals, can address the shortcomings and limitations of existing techniques to enhance water solubility. Drug nanocrystals are defined as nanoscopic crystals of parent substances measuring less than 1 micron [3]. Azelnidipine is absorbed in a dose-dependent manner when taken orally. As a BCS Class II drug, it has low solubility and high permeability. The bioavailability of Azelnidipine is less than 50%, indicating low bioavailability. Therefore, increasing the bioavailability, solubility, and dissolution rate of Azelnidipine is recommended. To overcome this problem, nanocrystals of Azelnidipine were prepared. [4].

In this study, the antisolvent precipitation method was used to prepare Azelnidipine nanocrystals. The dissolution and solubility behaviors were tested to confirm the enhancement. The crystalline form of AZL was investigated to increase its solubility and dissolution rate. The formulations were optimized with surfactants, such as sodium lauryl sulfate, and polymers, such as PVP K30, thereby further increasing solubility and dissolution rate. In vivo studies suggest that reducing particle size may limit the augmentation of dissolution rate benefits in nanoparticle systems [5].

Nanocrystals are drug particles that are stabilized with polymers or surfactants and have an average diameter of less than 1 μm. Generally, Nanocrystals are prepared by micro precipitation and high-pressure homogenization [6]. Azelnidipine is bright yellow, slightly bitter, and odorless. It is insoluble in water but soluble in ethanol. The present study aimed to develop and characterize nanocrystals of Azelnidipine, a poorly water-soluble BCS Class II drug, to enhance its solubility and dissolution rate. The research also includes a comprehensive preformulation study to evaluate the physicochemical properties of Azelnidipine. Nanocrystals were prepared by precipitation and subsequently optimized with respect to critical formulation parameters. Characterization will be performed using various analytical and physicochemical techniques to assess particle size, morphology, crystallinity, and stability. Furthermore, the in vitro drug-release profile of the optimized nanocrystal formulation will be compared with that of a conventional marketed product to assess its performance enhancement. In contrast to existing methods, the antisolvent precipitation method for creating Azelnidipine nanocrystals is novel because it employs a straightforward bottom-up approach that leverages differences in solvent and antisolvent solubility to produce pure, excipient-free nanoparticles with controlled size and shape.

By altering process variables such as flow velocity, drug concentration, solvent-antisolvent ratio, and pH, which affect nucleation and crystal development, this technique produces nanocrystals with exceptional uniformity and stability while enabling exact control over particle size [7]. Solid Lipid Nanoparticles (SLNs) and other crystallization or grinding techniques are examples of traditional technologies that frequently employ stabilizers or surfactants and may not provide fine control over particle-size distribution, potentially resulting in larger particles [6, 7]. Therefore, Azelnidipine nanocrystals with improved surface charge and crystalline structure may be produced efficiently and reproducibly via antisolvent precipitation. This could potentially improve the solubility, bioavailability, and therapeutic efficacy.

MATERIAL AND METHODS

Material

Azelnidipine was purchased from Moleculochem Laboratories Pvt Ltd, Ahmedabad, Gujarat (India). Sodium lauryl sulfate (SLS) and Polyvinylpyrrolidone K30 (PVPK30) were purchased from Nalkande distributors, Newasa, Maharashtra (India). Ethanol was purchased from MSSK Sonai (Maharashtra, India).

Method

Preparation of azelnidipine nanocrystals by the precipitation method

Azelnidipine nanocrystals were prepared by antisolvent precipitation [7]. Azelnidipine was thoroughly dissolved in Ethanol (10ml) using a magnetic stirrer at 1000 rpm for 30 min. (Solution no. 1). The stabilizing agents Tween 80 and PVPK-30 were dissolved in double-distilled water (100ml) (Solution 2). Solution no.2 was mixed at a constant speed of 1400 rpm using a propeller mixer for 30 min. Solution 1 was injected dropwise into solution 2 using a 25 mm syringe at a rate of 10 drops per minute (gtt /min) at room temperature. The addition of a solvent to a non-solvent caused drug precipitation. After stirring for 2 h, the mixture was centrifuged at 10,000 rpm for 10 min at 4 °C, then suspended in distilled water before sonication for 10 min. After sonication, the suspension was filtered under vacuum, then

dried for 24 h at 70°C. Controlling particle shape and adding stabilizers, such as sodium lauryl sulfate, can prevent particles from growing to micrometer size [8].

Experimental design

The nanocrystal formulation was optimized using a Box-Behnken design, a 3-factor, 2-level design, to analyze the effects of predefined independent variables on the quadratic response surface [9**]**. PVPK30 (Polyvinyl Pyrrolidone K30) and SLS (Sodium lauryl sulphate) were considered as independent variables, while Zeta potential, Polydispersity index, and mean particle size were dependent variables. Table 1 shows the formula composition of Azelnidipine nanocrystals.

Table 1: Formula composition with dependent and independent variables

	Independent variables (X)			**Dependent variable (Y)**		
Formulation code	**PVPK30 (A) (gm)**	**SLS (B) (gm)**	**Azelnidipine (gm)**	**Mean particle size (nm)**	**Polydispersity index (nm)**	**Zeta potential (mv)**
F1	0.1	0.05	0.1	124.6	0.570	-18.1
F2	0.1	0.10	0.1	201.4	0.648	-18.9
F3	0.1	0.150	0.1	119.2	0.749	-17.9
F4	0.2	0.05	0.1	201.1	0.635	-21.5
F5	0.2	0.10	0.1	212.3	0.741	-22.4
F6	0.2	0.150	0.1	165.3	0.605	-19.7
F7	0.3	0.05	0.1	204.6	0.558	-25.5
F8	0.3	0.10	0.1	215.6	0.741	-23.2
F9	0.3	0.150	0.1	199.6	0.655	-20.1

Characterization of Azelnidipine Nanocrystal

Determination of particle size, PDI, and zeta potential

A Zetasizer instrument and Dynamic light scattering (DLS) were used to measure particle size, PDI, and zeta potential [10].

UV spectroscopy

A UV-1800 Shimadzu spectrophotometer (Japan) was used to measure UV-visible spectra from 200 to 400 nm to check the absorbance of AZL Nanocrystals. The Nanocrystals were dispersed in distilled water and sonicated for 15 min before UV spectroscopic analysis.

Scanning electron microscopy (SEM)

The morphology of the drug-loaded nanocrystals was evaluated using a Shimadzu-60 in high-vacuum mode.

Fourier-transformed infrared spectroscopy (FTIR)

FTIR was used to assess the compatibility between the drug and the excipients in the formulation. IR spectra were recorded using the KBr pellet approach on FTIR in the wavelength range of 4000 to 400 cm^{-1}. The spectra of the drugs, polymers, and their physical combinations were compared.

Differential scanning calorimetry (DSC)

Drug and drug-loaded nanocrystals were analyzed for thermal characteristics and composition using DSC. The model employed was the LINSIES STP PT-1000, with a heating rate of 10℃ /min under ambient air conditions.

Physical state characterization using XRD:

The Physical state of the nanocrystals was examined using X-ray diffraction (XRD).

***In vitro* drug release from nanocrystals:**

Azelnidipine and Azelnidipine nanocrystals were tested for in vitro drug release utilizing a USP type I dissolution apparatus (basket type). The dissolution medium consisted of 900 mL of phosphate buffer at pH 6.8. The median temperature was maintained at 37 ± 0.5 °C. At different time intervals (0.25, 0.5, 1, 2, 4, 6, 8, 10, 12 h), 50 µL of material was withdrawn, centrifuged, and filtered using Whatman filter paper. The same amount of sample was used to replace the fresh dissolving media each time. Samples were examined at 256 nm in 0.1 N hydrochloric acid and 376 nm in phosphate buffer**.** A UV spectrophotometer was used to determine the drug concentrations in the samples. The cumulative drug release was determined [11].

Statistical analysis

A three-factor, three-level Box–Behnken Design (BBD) was employed to optimize the formulation of Azelnidipine nanocrystals. The experimental design was generated and

analyzed using Design-Expert® software (Stat-Ease Inc., Minneapolis, USA). The independent variables selected were PVP K30 concentration (A), Sodium lauryl sulfate (B), and homogenization speed (C), each studied at three coded levels (−1, 0, +1). The dependent variables (responses) were mean particle size (Y_1), polydispersity index (Y_2), and zeta potential (Y_3).

The obtained data were fitted to a second-order polynomial (2FI) model, and statistical analysis was performed using analysis of variance (ANOVA) to evaluate the significance of main, interaction, and quadratic terms. Model adequacy was assessed using parameters such as F-value, p-value, correlation coefficient (R^2), adjusted R^2, predicted R^2, and adequate precision. Three-dimensional response surface and contour plots were generated to visualize the interactive effects of formulation variables on each response and to identify the optimized formulation conditions. The optimized batch was further characterized for physicochemical properties and compared with the predicted model values to validate the design.

RESULTS AND DISCUSSION

Characterization of nanocrystal

UV spectroscopy

The spectra of nanocrystals showed an absorption peak in the 250-300 nm range. Azelnidipine (Drug) peak was found at 256 nm, indicating pure Azelnidipine (Figure 1).

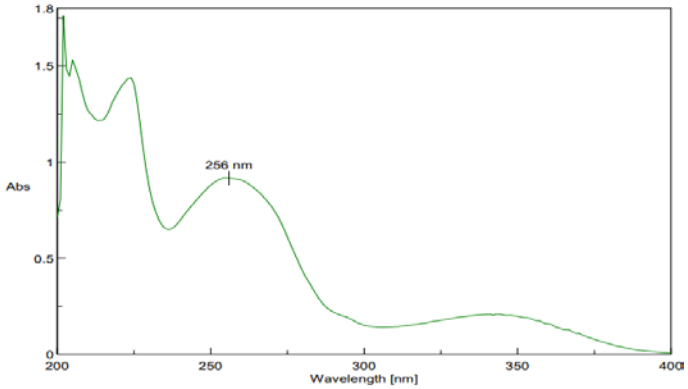

Figure 1: UV spectrum of Azelnidipine nanocrystals dispersed in solvent distilled water

Particle size, Polydispersity index (PDI), and zeta potential:

Determination of Particle size, PDI, and zeta potential was done using the ZetaSizer instrument. The particle size ranged between 119.2 and 215.6 nm, while the zeta potential ranged between -17.9 and -25.5 mV, and PDI ranged between 0.558 and 0.749. PDI of 1 indicates a perfectly uniform sample with all molecules having the same molecular weight. A PDI greater than 1 indicates a broader molecular-weight distribution. The PDI quantifies the width of the particle-size distribution. PDI is the ratio of the weight-average molecular weight (Mw) to the number-average molecular weight (Mn). It lacks a unit of measurement [12]. The comparative particle size, PDI, and zeta potential are presented in Table 2.

Table 2: Particle size, PDI, and zeta potential

Formulation code	Particle size(nm)	PDI	Zeta potential (mv)
F1	124.6	0.570	-18.1
F2	201.4	0.648	-18.9
F3	**119.2**	**0.749**	**-17.9**
F4	201.1	0.635	-21.5
F5	212.3	0.741	-22.4
F6	165.3	0.605	-19.7
F7	204.6	0.558	-25.5
F8	215.6	0.741	-23.2
F9	199.6	0.655	-20.1

The relatively high PDI values (0.558–0.749) indicate a moderately broad particle size distribution among the prepared nanocrystals. This may be attributed to variations in nucleation and growth rates during antisolvent precipitation and to the stabilizer concentration used. Although a lower PDI (<0.3) indicates a more uniform system, values below 0.8 are considered acceptable for nanosuspensions prepared by precipitation techniques. Such PDI values suggest moderate heterogeneity but still indicate good physical stability and acceptable uniformity for nanocrystal formulations. Based on particle size, zeta potential, and PDI, the optimized batch was identified as F3; the results are presented in Figures 2 and 3.

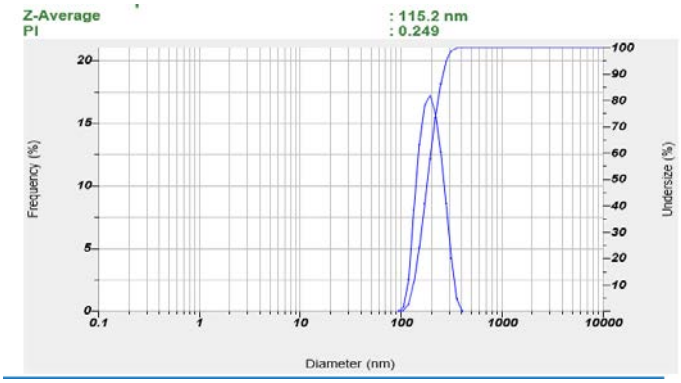

Figure 2: particle size and PDI of F3 batch

ANOVA for the 2FI model

ANOVA for the 2FI model of particle size showed a statistically significant effect, with an F-value of 111.67 (p = 0.0089), indicating that the probability of obtaining such a large F-value

by chance is less than 1%. Among these factors, polyvinyl pyrrolidone K30 (A), Sodium lauryl sulfate (B), Homogenization speed (C), as well as the AC and BC interaction terms, were found to be significant contributors to particle size ($p < 0.05$). In contrast, the AB interaction was not significant ($p = 0.1794$). These results suggest that particle size is strongly influenced by the main effects of A, B, and C, and by their interactions AC and BC, whereas the interaction between A and B has minimal impact. The model adequately explains the variability in particle size, and the non-significant terms could be removed to further refine the model.

Fit Statistics

Table 3: Fit statistics of particle size

Std. Dev.	6.01		**R^2**	0.9970
Mean	193.63		**Adjusted R^2**	0.9881
C.V. %	3.11		**Predicted R^2**	0.8335
			Adeq Precision	37.7893

Final Equation in Terms of Coded Factors

Particle Size (nm) = 204.98−48.00A+56.20B−24.70C −10.73AB+67.83AC−28.37BC

Final Equation in Terms of Actual Factors

Particle size = 1078.27 − 6370.05 (Polyvinyl pyrrolidone K30) + 6659.91 (SLS) − 1.036 (Homogenization speed -5.67409 Sodium lauryl sulphate * Homogenization speed

Counterplots and 3D surface plots showing the effects of independent variables on dependent variables are presented in Figures 4 and 5, respectively.

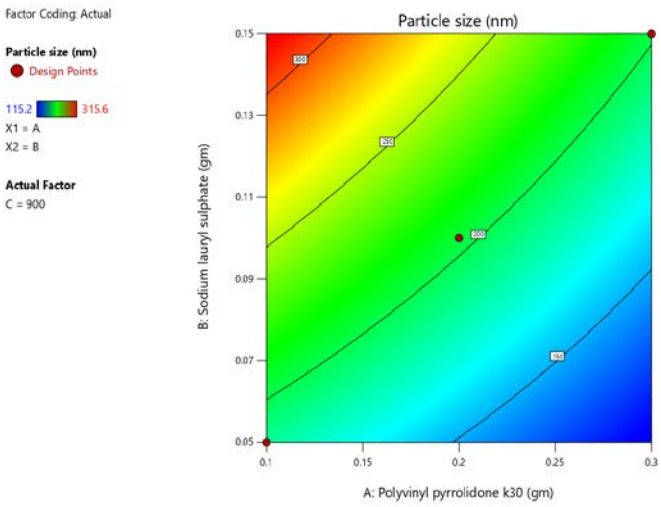

Figure 4: Counterplot showing the effect of independent variables on dependent variables

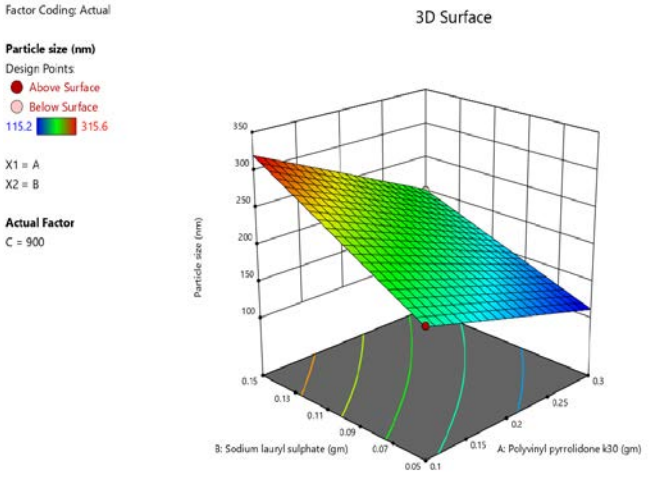

Figure 5: 3D Surface plot showing the effect of independent variables on dependent variables

ANOVA summary for particle size is given in below table 4

Table 4: ANOVA summary for particle size

Source	Sum of Squares	df	Mean Square	F-Value	p-Value	Significance
Model	6012.35	5	1202.47	111.67	0.0089	Significant
A-PVP K30	921.60	1	921.60	85.55	0.0112	Significant
B-SLS	1263.04	1	1263.04	117.12	0.0082	Significant
C-Homogenization speed	610.54	1	610.54	51.28	0.0183	Significant

Zeta potential:

ANOVA for the 2FI model

The ANOVA for the 2FI model of zeta potential indicated that the overall model was statistically significant, with a model F-value of 43.04 ($p = 0.0229$), suggesting that there is only a 2.29% probability that such a large F-value could arise by chance. Among the factors analyzed, Sodium lauryl sulfate (B), Homogenization speed (C), and the interaction terms AB and BC were significant contributors to zeta potential ($p < 0.05$). In contrast, polyvinyl pyrrolidone K30 (A) and the AC interaction were not significant ($p > 0.10$). These results indicate that zeta potential is primarily influenced by the main effects of B and C and their interactions with A, whereas A alone has minimal impact. The model effectively captures the variability in zeta potential, and non-significant terms may be considered for model refinement.

Fit Statistics

Table 5: Fit statistics of Zeta Potential

Std. Dev.	0.8190		**R^2**	0.9923
Mean	-18.69		**Adjusted R^2**	0.9693
C.V. %	4.38		**Predicted R^2**	0.8368
			Adeq Precision	23.1978

Final Equation in Terms of Coded Factors

Zeta Potential (mV)=−14.41−0.8386A−4.54B−3.95C−9.79AB+1.53AC+4.13BC

Final Equation in Terms of Actual Factors

Zeta Potential (mV)=+94.53409+49.977(PVPK30)−442.045 (SLS)−0.152614(Homogenization speed) – 1958.18182 Poly vinyl pyrrolidone k30 * Sodium lauryl sulphate +0.152727 Polyvinyl pyrrolidone k30 * Homogenization speed+0.825455 Sodium lauryl sulphate * Homogenization speed.

Counterplots and 3D surface plots showing the effects of independent variables on dependent variables are presented in Figures 6 and 7, respectively.

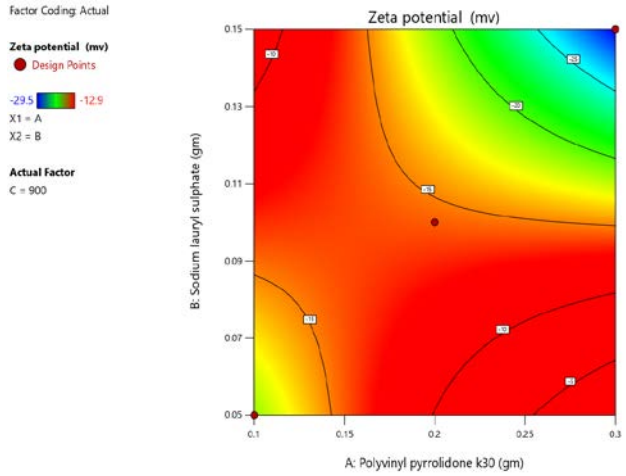

Figure 6: Counterplot showing the effect of independent variables on dependent variables

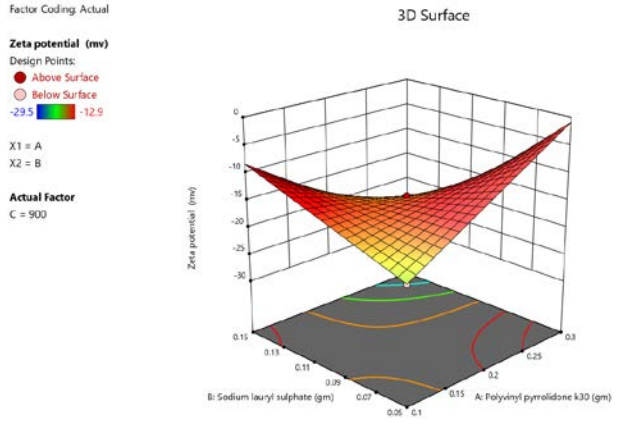

Figure 7: 3D Surface plot showing the effect of independent variables on dependent variables

Drug content and EE:

The drug content of formulations F1 to F9 varies from 75.68% to 97.46% **(Table 6)**. Formulation F3 has the highest drug content (97.46%), indicating superior drug loading or minimal degradation, whereas F7 has the lowest (75.68%), suggesting potential formulation or stability issues.

Table 6: Comparative drug content and EE

Formulation	Drug content (%)	EE (%)
F1	89.12	87.15
F2	92.45	89.45
F3	**97.46**	**95.45**
F4	85.46	82.43
F5	79.89	75.83
F6	86.28	84.23
F7	75.68	72.64
F8	90.18	88.20
F9	92.78	89.68

Formulations F2, F8, and F9, with drug contents of 92.45%, 90.18%, and 92.78%, respectively, are within an optimal range and may be suitable for further development. In contrast, formulations F4, F5, F6, and F7 may require further investigation and optimization to improve drug loading efficiency or stability. The entrapment efficiency of formulations F1 to F9 ranges from 72.64% to 95.45% **(Table 6)**. Formulation F3 exhibits the highest entrapment efficiency (95.45%), indicating effective drug encapsulation, whereas F7 has the lowest efficiency (72.64%), suggesting significant drug loss or leakage during formulation [13]. Formulations F2, F8, and F9 exhibit relatively high entrapment efficiencies, approaching 90%, indicating their potential for further development. However, formulations F4, F5, F6, and especially F7 may require optimization to enhance their entrapment capabilities and minimize drug loss [14].

Field Emission Scanning Electron Microscopy (FESEM):

The FESEM image (Figure 8) of the optimized batch F3 at 2,000× magnification shows distinct, well-defined particles with sharp edges and an angular morphology (Figure 8). Although such features are often associated with crystalline materials, FESEM alone cannot conclusively confirm crystallinity. The observed surface features may also result from particle aggregation during drying. Therefore, the crystalline nature of the nanocrystals was further confirmed by XRD, which provided direct evidence of the crystalline form of Azelnidipine in the optimized batch.

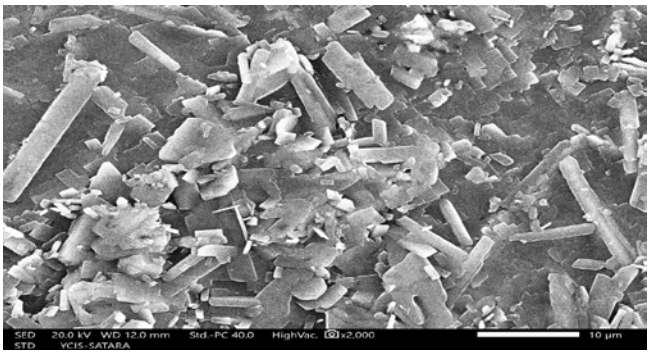

Figure 8: FESEM of optimized batch F3 at 2,000x

FTIR

The FTIR spectrum showed all characteristic functional groups of the drug, confirming its structural integrity. A broad band at 3660.23 cm^{-1} and 3372.89 cm^{-1} indicated N–H stretching, while peaks near 3050 cm^{-1} and 2938.98–2840.63 cm^{-1} corresponded to aromatic and aliphatic C–H stretching. The C≡N peak confirmed the nitrile group at 2030.68 cm^{-1}. Strong ester carbonyl peaks appeared at 1708.62 cm^{-1}, with aromatic C=C stretching at 1630.52 cm^{-1}. C–N stretching (1246.75 cm^{-1}), CH_3 bending (1375 cm^{-1}), C–O ester stretching (1287–1200 cm^{-1}), and C–O–C stretching (1101.15 cm^{-1}) were also observed. Additional aromatic out-of-plane and ring bending peaks at 981.59 and 751.13 cm^{-1} further confirmed the drug's identity. The FTIR spectrum of the optimized nanocrystal batch (F3) showed all major functional groups of the drug within their reported wavenumber ranges, confirming that the chemical structure remained intact after formulation. Key peaks included N–H stretching at 3705.55 cm^{-1} and 3679.51 cm^{-1}, the prominent peaks observed at 2971.77, 2921.63, 2864.74, and 2843.52 cm^{-1} represent aromatic and aliphatic C–H stretching (3000–3100 cm^{-1} and 2850–2960 cm^{-1}), nitrile C≡N peaks at 2360.44 (2210–2360 cm^{-1}), ester C=O stretching at 1709.59 cm^{-1}, and aromatic C=C at 1551.43, 1455.03 cm^{-1}. Additional C–N, C–O, and C–O–C vibrations also appeared within their expected ranges. Since no new peaks or major shifts were observed, the FTIR spectrum confirms that the drug is chemically stable and compatible within the optimized nanocrystal formulation shown in Figure 9.

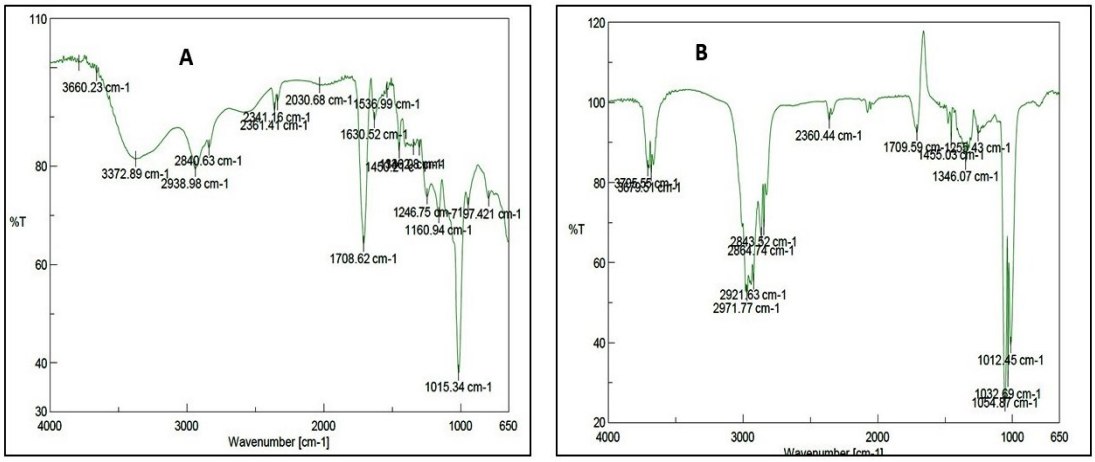

Figure 9: FTIR spectra of **(A) pure Azelnidipine and (B) optimized nanocrystal batch**

Differential scanning calorimetry

The DSC thermograms presented in Figure illustrate the thermal behavior of pure Azelnidipine (Figure 10A) and the optimized Azelnidipine nanocrystal formulation (Figure 10B). The pure drug exhibits a sharp endothermic peak at 128.88 °C, corresponding to its melting point, confirming its crystalline nature. In contrast, the nanocrystal formulation exhibits a slightly shifted and broadened endothermic peak at 125.00 °C. This shift to a lower temperature and the reduction in peak intensity indicate decreased crystallinity, which may be attributed to reduced particle size and possible partial Amorphization during nanocrystal preparation. Additionally, stabilizers such as PVP K30 and SLS may influence the melting behavior by interacting with drug molecules via hydrogen bonding or by reducing lattice energy [15]. Therefore, the observed shift likely results from a combined effect of decreased crystallinity, partial amorphous conversion, and stabilizer interactions, which together contribute to improved dissolution and bioavailability of Azelnidipine.

XRD analysis

The XRD pattern of pure Azelnidipine (Figure 11) shows a broad halo without sharp diffraction peaks, confirming its predominantly amorphous nature. In contrast, the optimized nanocrystal formulation (batch F3) displays multiple distinct and sharp diffraction peaks at 2θ values of 6.5°, 9.2°, 9.8°, 11.28°,

14.17°, 16.23°, 17.13°, 18.10°, 18.29°, 20.12°, and 22.25° (Figure 12), indicating a well-defined crystalline structure. The appearance of sharp peaks in the nanocrystal sample compared to the amorphous halo of the pure drug confirms a transition from amorphous to crystalline form during formulation. The high-intensity peaks, particularly at 2θ values of 9.2° and 14.17°, further support the presence of stable crystalline planes. This enhanced crystallinity may influence the dissolution rate and stability of the nanocrystals. The XRD findings are consistent with the FESEM and DSC results, which collectively confirm the crystalline nature of the optimized nanocrystals [16].

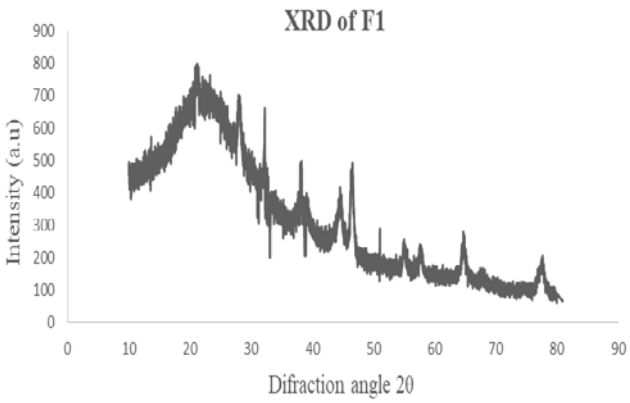

Figure 11: X-ray diffractometry of the Azelnidipine

***In vitro* Drug release profile of nanocrystals**

During the observation period, F3 emerges as the clearly optimized batch, exhibiting superior performance relative to the other factors (F1-F9). With F3 starting at 0 and steadily increasing over time, it consistently outstrips its counterparts, reaching its peak value of 95.68 at the 12-hour mark (Figure 13)

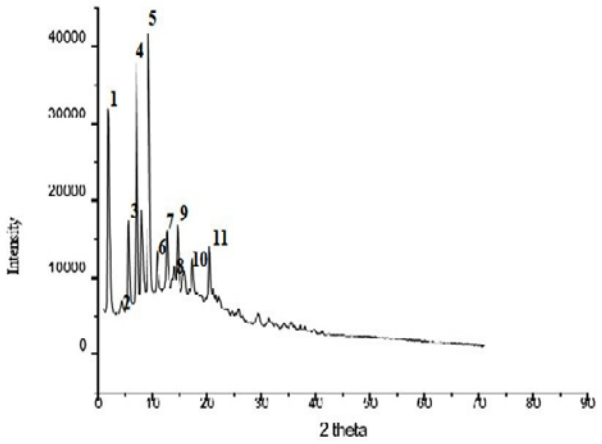

Figure 12: X-ray diffractometry of the optimized batch F3

Azelnidipine nanocrystals significantly increase drug release compared to the pure drug. The figure displays the cumulative percentage of drug released over time for various preparations. The cumulative percentage of drug released after 12 hours was 97.68, 87, and 92.25 for F3, F6, and F9. In contrast, pure Azelnidipine achieved a 37.66% rate at 60 minutes.

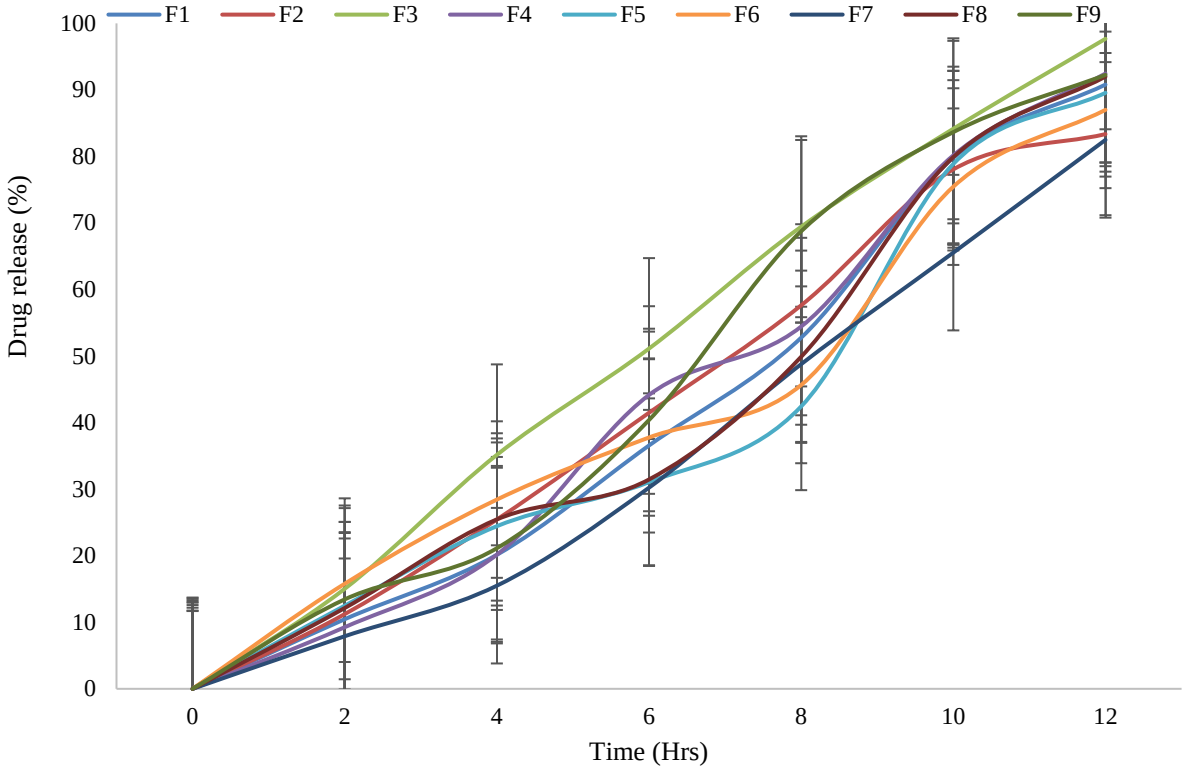

Figure 13: Comparative drug release profile

Formulations F3, F4, and F9 demonstrated the highest dissolving rates for PVPK30 and SLS polymers. In vitro release studies found that nanocrystals significantly increased the solubility of Azelnidipine compared with pure Azelnidipine. In vitro release profiles indicate that formulations F3, F4, and F9 exhibit higher dissolution rates than the other batches. Starting with batches F1 to F3, the drug-to-polymer PVPK30 ratio was 1:1, and the SLS concentration was increased to 0.05, 0.10, and 0.150. The highest drug release was observed in batch F3 (97.68%). F3 is selected as the optimized batch because it achieves the highest drug release. In batches F4 to F6, the drug-to-polymer PVPK30 ratio was 1:2, and the SLS concentration was 0.05, 0.10, or 0.150. In this case, the F4 batch showed the highest drug release, 92.46%. In batches F7 to F9, the ratio of drug to polymer PVPK30 was 1:3, and the concentration of SLS increased to 0.05, 0.10, and 0.150. In this case, the F9 batch shows the highest drug release, 92.25%. The study found that increasing the SLS concentration results in a faster dissolution rate.

Mechanism of dissolution enhancement

The enhanced dissolution of Azelnidipine from the nanocrystals can be readily explained by classical dissolution theory. According to the Noyes-Whitney equation,

$$\frac{dC}{dt} = \frac{DA}{hV}(C_s - C)$$

where dC/dt is the dissolution rate, D is the diffusion coefficient, A is the particle surface area, h is the thickness of the diffusion layer, V is the volume of dissolution medium, Cs is the saturation solubility, and C is the bulk concentration. Reduction of particle size to the nanometer range greatly increases the total surface area (A) available for dissolution. It often reduces the diffusion-layer thickness (h), thereby increasing the dissolution rate. In addition, the Ostwald–Freundlich relationship predicts that very small particles can exhibit an increased apparent solubility (Cs), promoting a higher driving force (Cs − C) for dissolution. The stabilizers used in the formulation (PVP K30 and SLS) further contribute by improving wetting, preventing particle aggregation, and maintaining a dispersed state that sustains the enlarged surface area and, in many cases, a transient supersaturated state. Together, these factors—increased surface area, possible elevation of apparent solubility for nanosized crystallites, and improved wettability/stabilization—explain the markedly faster and greater extent of drug release observed for the nanocrystals compared with the coarse drug.

ANOVA for linear model

The ANOVA results for the linear model of drug release indicate a statistically significant effect, with an F-value of 14.45 and a p-value of 0.0067, suggesting only a 0.67% probability that such a large F-value could occur by chance. Among the independent variables, polyvinyl pyrrolidone K30 (A) and homogenization speed (C) were identified as significant factors influencing drug release, with p-values of 0.0063 and 0.0394, respectively. While Sodium lauryl sulfate (B), although not statistically significant (p = 0.5867), contributed positively to the formulation stability and reproducible release. These findings indicate that modulation of PVP K30 and homogenization speed can effectively control drug release, with SLS supporting overall formulation performance.

Fit Statistics

Table 7: Fit statistics of drug release

Std. Dev.	1.95		**R^2**	0.8966
Mean	89.73		**Adjusted R^2**	0.8346
C.V. %	2.17		**Predicted R^2**	0.7079
			Adeq Precision	10.4027

Final Equation in Terms of Coded Factors

Drug Release=89.72+4.37A+0.5624B−2.39C

Final Equation in Terms of Actual Factors

Drug Release=101.33596+43.72372(Polyvinyl pyrrolidone K30)+11.24744(Sodium lauryl sulphate)−0.023878 Homogenization speed

The counterplot and 3D surface plots showing the effects of independent variables on dependent variables are presented in Figures 14 and 15, respectively.

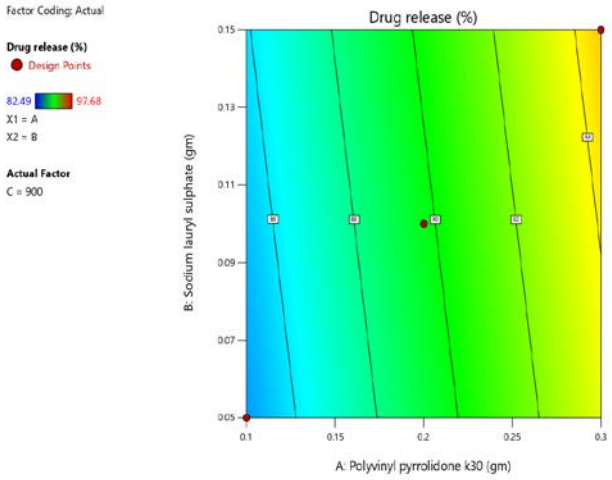

Figure 14: Counterplot showing the effect of independent variables on dependent variables

CONCLUSION

Antisolvent precipitation was found to be an effective method for reducing particle size. It can be used for a variety of drugs, depending on their physicochemical properties and the use of a suitable stabilizer. The study demonstrated that Azelnidipine maintains its crystalline state even after particle size reduction, indicating long-term stability.

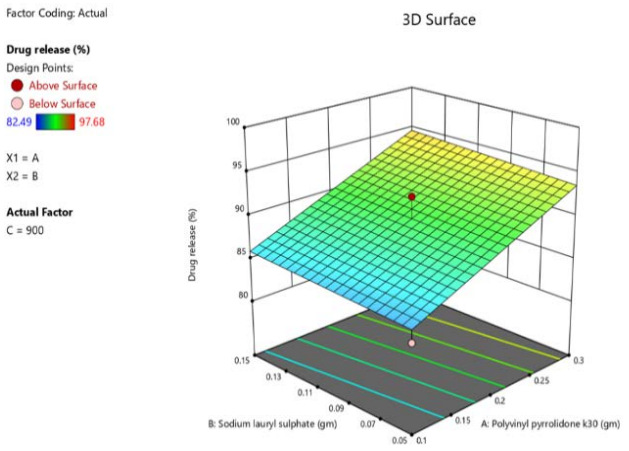

Figure 15: 3D Surface plot showing the effect of independent variables on dependent variables

The conversion of Azelnidipine from micronized to nanocrystal form significantly enhanced its solubility and dissolution rate. The improved dissolution behavior indicates a potential for increased oral bioavailability, as faster and more complete dissolution can enhance drug absorption in the gastrointestinal tract. Thus, the developed nanocrystal formulation represents a promising approach to overcome the solubility-limited bioavailability of Azelnidipine. Research indicates that an optimized nanocrystal formulation of Azelnidipine improves its solubility relative to the pure drug and existing formulations.

FINANCIAL ASSISTANCE

The authors express gratitude to the DIST-FIST Project (File no. DST FIST-2015; File No.SR/FST/College-272), Department of Science and Technology, New Delhi, Rajiv Gandhi Science and Technology Commission (RGSTC), Mumbai, and AICTE (All India Council for Technical Education) (MODROB) for their financial support in the central instrumentation facility at SRES, Sanjivani College of Pharmaceutical Education and Research (Autonomous), Kopargaon, India for this research work. The author acknowledges the contribution of "SAARTHI", an Autonomous Body of the Government of Maharashtra, for providing funding in the form of Junior Research Fellowship (JRF) for Research work.

CONFLICT OF INTEREST

The authors declare no conflict of interest.

AUTHOR CONTRIBUTION

Vipul P. Patel designed the study and planned the work, including its aims and objectives; reviewed the manuscript; and edited the article. Sandeep D. Kardile performed the work, collected data, and wrote the manuscript.

REFERENCES

[1] Mazayen ZM, Ghoneim AM, Elbatanony RS, Basalious EB, Bendas ER. Pharmaceutical nanotechnology: from the bench to market. *Pediatr Res*, **8**, 12 (2022) https://doi.org/10.1186/s43094-022-00400-0

[2] Sood R, Tomar D, Kaushik P, Sharma P, Rani N, Guarve K. Enhanced solubility and increased bioavailability with engineered nanocrystals. *Curr Drug Ther*, **19**, 638-647 (2024) https://doi.org/10.2174/0115748855269071231113070552

[3] Ghaferi M, Zahra W, Akbarzadeh A, Shahmabadi HE, Alavi SE. Enhancing the efficacy of albendazole for liver cancer treatment using mesoporous silica nanoparticles: an in vitro study. *EXCLI J*, **21**, 236 (2022) https://doi.org/10.21203/rs.3.rs-294729/v1

[4] Goba I, Turovska B, Belyakov S, Liepinsh E. Synthesis of novel unsymmetrically substituted 1,4 dihydroisonicotinic acid and its derivatives. *Chem Heterocycl Compd*, **49**, 726-735 (2013) https://doi.org/10.1007/s10593-013-1304-3

[5] Kumar R, Thakur AK, Chaudhari P, Banerjee N. Particle size reduction techniques of pharmaceutical compounds for the enhancement of their dissolution rate and bioavailability. *J Pharm Innov*, **17**, 333-352 (2022) https://doi.org/10.1007/s12247-020-09530-5

[6] Purohit D, Sharma S, Lamba AK, Saini S, Minocha N, Vashist N. Nanocrystals: a deep insight into formulation aspects, stabilization strategies, and biomedical applications. *Recent Pat Nanotechnol*, **17**, 307-326 (2023) https://doi.org/10.2174/1872210516666220523120313

[7] Wu W, Zu Y, Wang L, Wang L, Wang H, Li Y. Preparation, characterization and antitumor activity evaluation of apigenin nanoparticles by the liquid antisolvent precipitation technique. *Drug Deliv*, **24**, 1713-1720 (2017) https://doi.org/10.1080/10717544.2017.1399302

[8] Hafizah MA, Riyadi AF, Manaf A. Particle size reduction of polyaniline assisted by anionic emulsifier of sodium dodecyl sulphate (SDS) through emulsion polymerization. *IOP Conf Ser Mater Sci Eng*, **515**, 012080 (2019) https://doi.org/10.1088/1757-899X/515/1/012080

[9] Pantub K, Wongtrakul P, Janwitayanuchit W. Preparation of salicylic acid loaded nanostructured lipid carriers using Box-Behnken design: optimization, characterization and

physicochemical stability. *J Oleo Sci*, **66**, 1311-1319 (2017) https://doi.org/10.5650/jos.ess17051

[10] Ala Allah AK, Abd Alhammid SN. D α TPGS/poloxamer 188 mixed micelles for the oral delivery of azelnidipine: preparation and in vitro evaluation. *Al Mustaqbal J Pharm Med Sci*, **2**, 3 (2024) https://doi.org/10.62846/3006-5909.1012

[11] Dugad T, Kanugo A. Design optimization and evaluation of solid lipid nanoparticles of azelnidipine for the treatment of hypertension. *Recent Pat Nanotechnol*, **18**, 22-32 (2024) https://doi.org/10.2174/1872210517666221019102543

[12] Dwivedi SD, Singh D, Singh MR. A Piper nigrum based zinc oxide nanoparticles for anti-arthritic and antioxidant activity. *J Appl Pharm Res*, **12**, 51-59 (2024) https://doi.org/10.69857/joapr.v12i5.727

[13] Lokeshvar R, Ramaiyan V, Nithin V, Pavani S, Vinod Kumar T. Nanotechnology-driven therapeutics for liver cancer: clinical applications and pharmaceutical insights. *Asian J Pharm Clin Res*, **18(2)**, 8-26 (2025) https://doi.org/10.22159/ajpcr.2025v18i2.53429

[14] Soliman KA, Ibrahim HK, Ghorab MM. Effects of different combinations of nanocrystallization technologies on avanafil nanoparticles: in vitro, in vivo and stability evaluation. *Int J Pharm*, **517**, 148-156 (2017) https://doi.org/10.1016/j.ijpharm.2016.12.012

[15] Leng E, Zhang Y, Peng Y, Gong X, Mao M, Li X. In situ structural changes of crystalline and amorphous cellulose during slow pyrolysis at low temperatures. *Fuel*, **216**, 313-321 (2018) https://doi.org/10.1016/j.fuel.2017.11.083

[16] Chakole D, Rakte A, Pande V, Kothawade S, Suryawanshi J. Precision drug delivery through methotrexate. *J Appl Pharm Res*, **12**, 38-45 (2024) https://doi.org/10.69857/joapr.v12i3.528